Influence of mechanical and water-jet cutting on the dynamic magnetic properties of NO Fe-Si steels

Contents lists available at ScienceDirect

Journal of Magnetism and Magnetic Materials

journal homepage: http://ees.elsevier.com

Research articles

Influence of mechanical and water-jet cutting on the dynamic magnetic properties of NO Fe-Si steels

Veronica Manescu (Paltanea) [a], Gheorghe Paltanea [a,*], Enzo Ferrara [b], Iosif Vasile Nemoianu [a], Fausto Fiorillo [b], Horia Gavrila [a]

[a] Department of Electrical Engineering, University Politehnica of Bucharest, Bucharest, RO 060042, Romania
[b] Advanced Materials Metrology and Life Sciences, Istituto Nazionale di Ricerca Metrologica—INRIM, 10135 Torino, Italy

ARTICLE INFO

Keywords
Non-oriented electrical steel
Magnetic losses
Loss separation
Magnetization curve
Cutting technology
Strain-hardening

ABSTRACT

Magnetization curve and energy losses have been analyzed in non-oriented (NO) Fe-Si alloys with variable thickness (0.20 mm–0.35 mm), cut at widths ranging between 5 mm and 60 mm, in order to assess the impact of cutting, either done by punching or water-jet techniques. Measurements were performed by means of a digitally controlled single strip tester, from dc up to 1.5 kHz, at peak polarization values J_p = 1.0 T and 1.5 T. The evolution of the magnetization curve and the structure-dependent hysteresis W_h and excess W_{exc} loss components have been assessed as a function of the strip width using a simple phenomenological model, by which the extension of the damaged area at the edges of the cut sheets is estimated. Such a model assumes a hyperbolic dependence of the measured polarization on the cut strip width. The limiting values of W_h and W_{exc} for the fully damaged and the pristine sheets are in this way estimated, showing that one can simply and affordably predict the magnetic behavior of NO Fe-Si steels subjected to cutting.

1. Introduction

Understanding the magnetization process in non-oriented (NO) Fe-Si sheets is basic to the improvement of the performances of the electrical machines and the efficient conversion of the huge amount of energy fluxing through their magnetic cores worldwide [1,2]. Sheet cutting is a critical step in core manufacturing by fully processed NO steels, because the induced strain deteriorates the soft magnetic response of the material [3,4].

The various steps needed to optimize the magnetic properties of the steels pass through cold rolling, annealing, recrystallization, and decarburization [5–10], with possible addition of impurities, such as Sb and Sn, as well as Mn in very clean steels. These can induce selective growth of those recrystallized grains that have orientations close to the ideal random cubic texture {1 0 0} <0*vw*> [11,12].

At the end of the manufacturing process, however, cutting may affect the technological performance of the NO Fe-Si sheets and reduce the beneficial effects of the previous treatments. Mechanical punching is ubiquitously applied for lamination cutting. This process has obvious detrimental consequences on the magnetic properties, because of strain-hardening and ensuing non-uniform magnetization profile across the strip width [13–16].

Water-jet cutting, which combines high-pressure laminar water flows and abrasive particles for the erosion of the sheet, is accompanied by minimum deformation stresses. A more uniform profile of magnetic induction is therefore expected across the strips [17], but water-jet is only used in the prototyping production, because it is expensive and has a relatively slow cutting rate.

The subject of work hardening by cutting has attracted substantial efforts in the literature in recent years. These investigations have phenomenological character. Their aim, on the one hand, is to determine the extent of the structural damage, the residual stress, and the induction profile across the sample width, using, for example, neutron grating interferometry, [15,16,18–21]. On the other hand, they are generally directed at relating the cutting methods, including laser cutting, and the related parameters to the behavior of the total loss at power frequencies, with the final objective of introducing the results in the calculation of iron losses in rotating machines [13,14]. However, the physical problem cannot be satisfactorily investigated, and simple predictions cannot be formulated without being inquisitive about the role and behavior of the loss components (hysteresis, classical, excess) and their individual response to the cutting-induced strain hardening. Each component depends in fact in a specific way on frequency and peak induction, on sample geometry and material treatment. This kind of approach is conspicuously lacking in the literature.

In this paper, we investigate the evolution of the magnetization curve and of the energy loss and its components versus frequency in punched and water-jet cut Fe-Si sheets 0.20 mm and 0.35 mm thick. Following prior experiments on the hysteresis loss [22,23] we focus on the excess loss component, the quantity characterizing the degree

Corresponding Author:
E-mail address: gheorghe.paltanea@upb.ro (G. Paltanea)

https://doi.org/10.1016/j.jmmm.2019.166257
Received 8 August 2019; Received in revised form 27 October 2019; Accepted 30 November 2019
Available online xxx
0304-8853/

of damping of the domain wall (dw) motion by the mesoscopic eddy currents. We obtain that magnetic hardening by cutting can be quantified in terms of simple hyperbolic laws, describing the measured polarization J_p, the hysteresis loss W_h, and the excess loss W_{exc} as a function of the strip width.

2. Materials and methods

The investigated NO Fe-Si strip samples with thickness $d = 0.20$ mm (Cogent NO20 Hi-Lite) and 0.35 mm (Cogent M300-35A) were cut along the rolling direction (RD) from parent sheets by punching and water-jet stream, at widths $w = 5$–60 mm and length 300 mm. The density of the alloys is $\delta = 7650$ kg/m^3 and the electrical resistivity is $52{\cdot}10^{-8}$ Ωm and $50{\cdot}10^{-8}$ Ωm in the NO20 and M300-35A steel sheets, respectively. While crystallographic investigations were not within the scope of this work, the magnetic measurements, made according to the standards, with mixed RD and TD Epstein strips, point to 10%–15% anisotropy of magnetic losses in these non-oriented materials. The specific direction of sheet cutting appears therefore irrelevant from the viewpoint of the cutting-induced magnetic hardening. The average grain size is 122 μm and 86 μm in the NO20 and M300-35A steel sheets, respectively.

In the case of punching, the guillotine method was chosen, and an industrial shear-cutting tool was involved. The most important tool parameter is the cutting clearance, which represents the distance between the punch and die, set at 35 μm. The punch was a normal tool, whose radius is estimated between 30 μm and 50 μm. The surface pressure under the blank holder is 250 MPa. In the case of water-jet cutting technology, we have used an industrial water-jet device supplied by a high-pressure pump of 40 MPa, which uses a mixture of Garnet 80 mesh particles with density of 4100 kg/m^3 and average diameter 0.18 mm. It has a 0.4 mm diameter sapphire orifice with a carbide nozzle of 1.05 mm diameter for the abrasive water jet. The cutting conditions were the same for both types of electrical steel. The magnetic measurements were made by means of a calibrated hysteresisgraph endowed with digital control of the induction waveform [24]. The magnetic field was applied by means of a flat wide solenoid, inserted, together with the measuring strips, between the pole faces of a vertical double-C laminated yoke. The strips, from 12 to 1, were placed side-by-side, in order to always form a 60 mm wide testing sample. Besides the normal magnetization curve, the energy loss $W(f)$ was measured for $J_p = 1.0$ T and 1.5 T up to 1500 Hz and 400 Hz in the 0.20 mm thick and 0.35 mm thick strip samples, respectively.

The procedure of loss decomposition, passing through the analysis of the statistics of the "magnetic objects" [25], shows that these are the upper frequencies attainable without incurring into non-negligible skin effect.

3. Results and discussions

3.1. Normal magnetization curves

The influence of the cutting procedure on the quasi-static normal magnetization curve, obtained as the locus of the tip points of a sequence of symmetric hysteresis loops, taken up to the maximum peak field $H_p = 5$ kA/m, is shown for the 0.20 mm thick NO Fe-Si sheets in Figs. 1 and 2. The evolution of the curve upon the decrease of the strip width from 60 mm to 5 mm puts in evidence how magnetic hardening is reduced in the water-stream cut samples.

The inset of Fig. 1 provides a schematic subdivision of the cut strip into an undamaged core and two strain-hardened lateral bands of width L_c. This rather crude model, where the measured peak polarization J_p is the weighted average of polarization value attained in the core J_{p0} and the one pertaining to the damaged bands J_{pc}, provides, for any given applied field H the dependence of J_p on the strip width w as:

$$J_p(w) = J_{p0} - (J_{p0} - J_{pc})\frac{2L_c}{w}, (w \geq 2L_c) \quad (1)$$

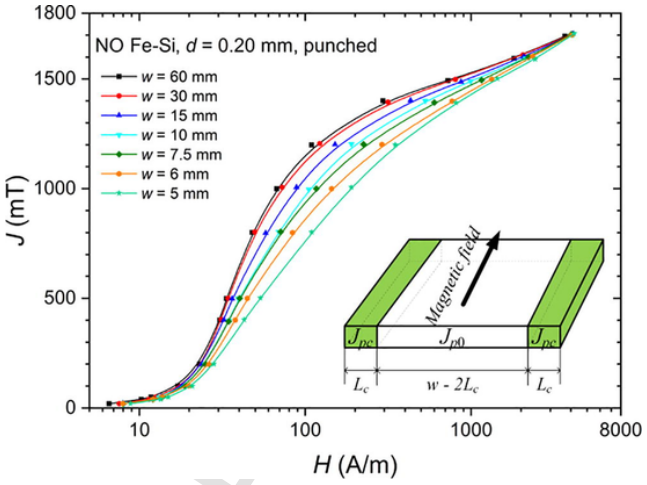

Fig. 1. Quasi-static normal magnetization curves versus width w of the strip samples in punched 0.20 mm thick NO Fe-Si strips. The scheme in the inset provides a coarse model for the cut strip, endowed with damaged lateral bands of width L_c, and a central unscathed region.

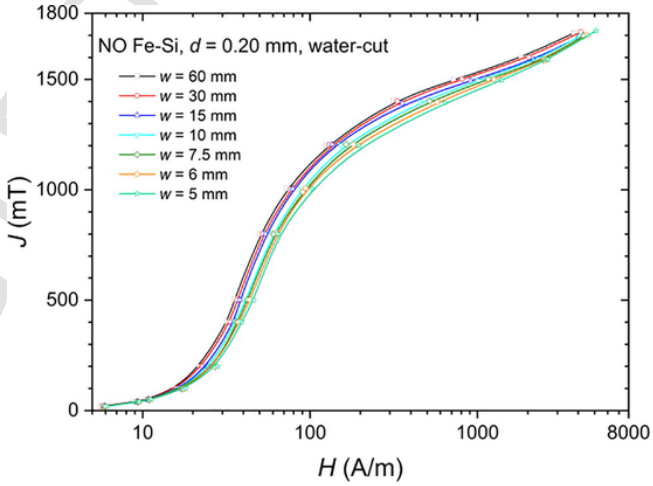

Fig. 2. Same as Fig. 1 for the water-jet cut 0.20 mm thick NO Fe-Si strips.

where J_{pc} and J_{p0} (with $J_{pc} \leq J_{p0}$) are the polarization values belonging to the two strain-hardened bands and the central undamaged region of width $w - 2L_c$, respectively.

Let us write, for a defined applied field value H, Eq. (1) as $J_p(w) = a - b/w$. By measuring the magnetization curve at two generic strip widths (for example $w_1 = 30$ mm and $w_2 = 10$ mm), J_{pc} and J_{p0} are found for any H value and we obtain the parameters $a(H)$ and $b(H)$. This permits us to predict the J_p versus w curves shown in Fig. 3 for the 0.20 mm thick water-jet cut strips at defined H values (50 A/m $\leq H \leq$ 5 kA/m). As similarly observed in previous experiments on punched strips [22,23], Eq. (1) provides excellent fitting of the experimental $J_p(w)$ behaviors (symbols). We can immediately conclude from the saturating behavior of these curves on increasing w, that the effect of water-jet cutting becomes negligible for $w > 40$–50 mm. By the same fitting curves, we can estimate the width of the fully damaged bands. Such an estimation, signaled by the straight vertical line in Fig. 3, is made, on the one hand, by identifying the $a(H)$ and $b(H)$ parameters at very high fields, where all the curves eventually coalesce and $b(H)$ tends to zero, and on the other hand, by the obvious condition $J > 0$ at the lowest H values. We thus evaluate $2L_c \sim 3.0$ mm in the water-jet cut 0.20 mm thick laminations (vertical line in Fig. 3). The intersection points of this line with the $J_p(w)$ curves predicted by Eq. (1) identify the magnetization curve of the strain-hardened lateral bands.

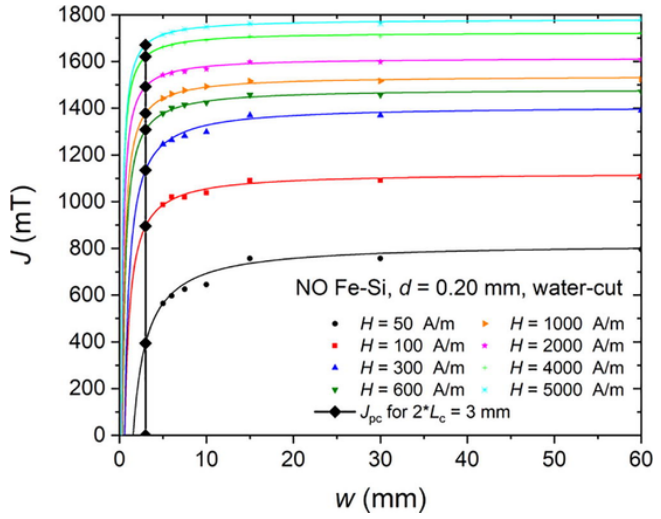

Fig. 3. Magnetic polarization J (symbols), measured at different field strengths in the 0.20 mm NO Fe-Si water-cut samples, as a function of strip width w. The solid lines are predicted by the hyperbolic function (1). The vertical line identifies the estimated width $w = 2L_c$ of the fully damaged strip.

The same procedure works in the case of 0.35 mm thick alloys cut either by punching or water-jet stream. Table 1 shows the so-found values of $2L_c$ in the investigated materials. The uncertainty of such estimate is evaluated around ±10%–20%.

3.2. Quasi-static energy loss

The hysteresis energy loss W_h is obtained by extrapolating to $f \to 0$ the measured $W(f)$. This quantity has obvious physical meaning, because it is identified with the energy dissipated by the localized discontinuities of the dw motion (Barkhausen jumps). Because of its local nature, we can treat $W_h(w)$ as we did with the polarization $J_p(w)$ and write

$$W_h(w, J_p) = W_{h0}(J_{p0}) + (W_{hc}(J_{pc}) - W_{h0}(J_{p0}))\frac{2L_c}{w}, (w \geq 2L_c) \quad (2)$$

where W_{hc} and W_{h0} (with $W_{hc} \geq W_{h0}$) are the specific loss values associated with the strain-hardened and the core regions, respectively. By taking again the two strips of width w_1 and w_2 and using the related experimental $W_h(w, J_p)$ curves, we find $W_h(w_1, J_p(H_p))$ and $W_h(w_2, J_p(H_p))$ for a same H_p value, we solve Eq. (2) for $W_{hc}(J_{p0})$ and $W_{hc}(J_{pc})$, and we arrive at the dependence of $W_h(J_p)$ on the strip width. Predicting examples by Eq. (2) are provided for $J_p = 1.5$ T and 1.0 T (solid lines) in Fig. 4, compared with the experimental $W_h(w)$ values (symbols).

The strip width $w = 2L_c$ at which the strip appears to be fully strain-hardened by cutting, corresponding to the upper limit $W_h(2L_c, J_p)$ for the hysteresis loss, is signaled (diamond symbols). The advantage of water-jet cutting in terms of reduced additional losses is apparent.

Table 1
Estimated values of the width $2L_c$ of the degraded portion of the cut Fe-Si strips (see Fig. 1). It corresponds to the width of a fully damaged strip.

Thickness d (mm)	Punched	Water-cut
0.20	3.5 mm	3 mm
0.35	4 mm	3 mm

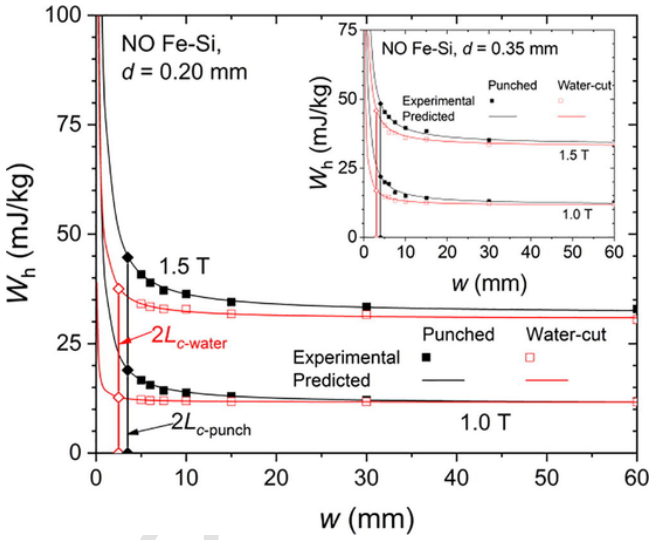

Fig. 4. Hysteresis loss W_h versus cut strip width w measured at $J_p = 1.0$ T and 1.5 T in the 0.20 mm and 0.35 mm (inset) thick NO Fe-Si alloys (symbols) and their prediction by Eq. (2) (solid lines). The lower limiting width $w = 2L_c$ of the fully damaged material is signaled by the diamond symbols.

3.3. Dynamic losses

The dynamic magnetic properties of the differently cut NO Fe-Si strips have been analyzed by loss decomposition, as sketched in Fig. 5, according to the Statistical Theory of Losses [25].

The classical energy loss $W_{cl}(f)$ is readily calculated, because, being chiefly associated with the macroscopic eddy currents, for the great part confined at and close to the sheet surface, they mostly descend from the rate of change of the flux throughout the whole sample cross-section, that is, from

the average polarization value J_p. We can then write, in the absence of skin effect [26], for a strip of thickness d, resistivity ρ, and density δ

$$W_{cl}(f) = (\pi^2/6)\cdot\left[d^2 J_p^2 f/(\rho\delta)\right], [J/kg] \quad (3)$$

a quantity not affected by cutting.

Of course, $W_{cl}(f)$ provides for a part only of the dynamic losses, whose complete analysis requires modeling of the excess loss $W_{exc}(f)$, experimentally obtained as

$$W_{exc}(f) = W(f) - W_h(f) - W_{cl}(f). \quad (4)$$

Fig. 5a and 5b show the measured behaviors of $W(f)$ at $J_p = 1.5$ T in the water-cut and punched 0.20 mm thick strips up to $f = 1500$ Hz The $W_{exc}(f)$ curves extracted from $W(f)$ using Eq. (4) are shown for the different strip widths in Fig. 5. It is observed that both hysteresis and excess losses increase with decreasing the strip width, that is, by increasing the average magnetic hardness caused by plastic deformation. It is also apparent that $W_{exc}(f)$ follows an $f^{1/2}$ dependence. We can actually describe this behavior taking advantage of the formulation given by the Statistical Theory of Losses, which provides on very general grounds [27]

$$W_{exc}(f) = 2n_0 V_0 J_p \int_0^{\pi/2}\left(\sqrt{1 + \frac{8GS_t V_0}{\rho n_0^2 V_0^2}\pi f J_p \cos\phi} - 1\right)\cos\phi d\phi, \quad (5)$$

for sinusoidal induction. S is the cross-sectional area, $G = 0.1356$, and the statistical parameters, n_0 and V_0 refer to the discrete structure of the magnetization process and the statistics of the local coercivities

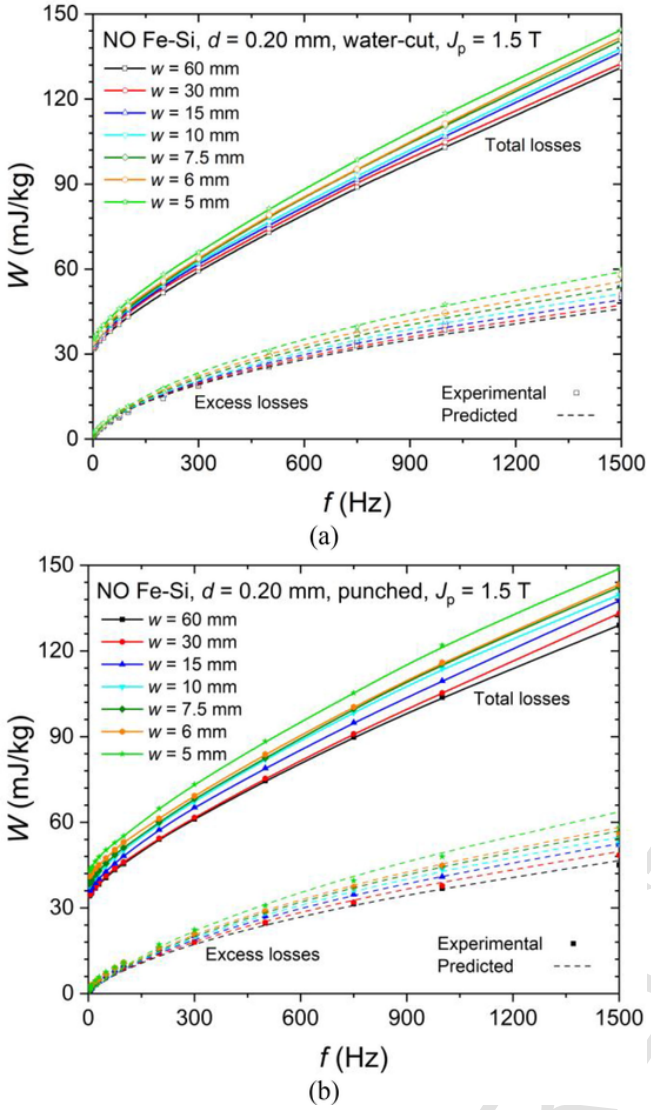

Fig. 5. Energy loss $W(f)$ measured versus frequency at J_p = 1.5 T in water-cut (a) and punched (b) 0.20 mm thick NO Fe-Si strips. The strip width ranges between 5 mm and 60 mm. The excess loss component $W_{exc}(f)$ is extracted from $W(f)$ according to Eq. (4). The dashed lines show fitting of $W_{exc}(f)$ by means of Eq. (5).

(see [28]). The fitting lines in Fig. 5 are calculated by Eq. (5) using single values for n_o and V_0. These values play the role of an average of the actual parameters pertaining to the cold-worked bands and the core. As expected, the parameter V_0, approximately proportional to the coercive field, increases with decreasing the width w.

The term $W_{exc}(f)$ lumps the energy dissipated by the eddy currents circulating in the immediate surroundings of the moving domain walls. The local character of these currents makes it possible to distinguish between the contributions to $W_{exc}(f)$ provided by the strain-hardened bands and the pristine core of the strip. Consequently, by further taking into account, as previously stressed, that hysteresis and excess losses are physically related [25], we are naturally led to generalize Eq. (2) to the behavior of the excess loss and write its dependence on the strip width at any frequency f as

$$W_{exc}(w, J_p, f) = W_{exc}(J_{p0}, f) + \left(W_{exc}(J_{pc}, f) - W_{exc}(J_{p0}, f)\right)\frac{2L_c}{w}, \quad (6)$$

with $W_{exc}(J_{p0}, f)$ and $W_{exc}(J_{pc}, f)$ associated with the core and the lateral bands, respectively. By repeating, although to somewhat higher degree of approximation, the procedure previously described for $W_h(w, J_p)$ and using, for any given frequency f, the experimental $W_{exc}(w, J_p)$ curves at widths w_1 and w_2, we find $W_{exc}(w_1, J_p(H_p))$ and $W_{exc}(w_2, J_p(H_p))$ for the same H_p value. We introduce these quantities in Eq. (6) and we obtain $W_{exc}(J_{p0}, f)$ and $W_{exc}(J_{pc}, f)$, by which the excess loss $W_{exc}(w, J_p, f)$ for any width w can be predicted.

The continuous lines in Fig. 6 show the so-calculated dependence of W_{exc} (f = 50 Hz, J_p = 1.0 T and 1.5 T) in the NO Fe-Si, 0.20 mm thick sheet, as a function of w. The experimental results (symbols) are obtained in the punched and water-jet cut samples. As predicted by the theory [25,28], the increase of coercivity and hysteresis losses by mechanical hardening is paralleled by an increase of the excess losses.

4. Conclusions

We have investigated the effect of cutting on the magnetization curve and magnetic losses of NO Fe-Si steels of different thickness (0.20 mm and 0.35 mm) and we have worked out a simple model to consider the overall phenomenology from dc up to 1.5 kHz. The proposed approach permits one to assess the role of punching and water-jet cutting on the quasi-static and dynamic energy loss behavior, in conjunction with the loss decomposition method. This is accomplished by using simple analytical expressions.

Starting from an elementary scheme, where narrow work-hardened bands at the edges of the cut strips are distinguished from the undamaged inner core, it is predicted and experimentally observed that, under defined applied field H, the polarization level $J(H)$, hysteresis loss $W_h(J_p)$, and excess loss $W_{exc}(J_p)$ at given peak polarization, J_p, all follow hyperbolic dependences on the width w of the cut strip samples. The width of the plastically strained band at each strip edge is also estimated, by means of fitting. It turns out to be of the order of 1.5–2 mm, with increased damage observed in the guillotine-punched strips. It is finally observed that hysteresis loss and excess loss follow similar increasing trends upon increased mechanical hardening. This confirms the theoretical expected correlation between the material coercivity and the statistics of the dw dynamics in NO steel sheets.

There is no reason to limit the developed model to strips and straight cutting lines. Once a certain cutting procedure is defined on such samples, more complex profiles, as the ones found with teeth and slots in stator cores, can be treated in the same way, with some possible limitations in corner zones, where the distribution of the residual stresses is complex. The model is quite general and can be appropriately applied to the laser cutting technology, independent of the differ-

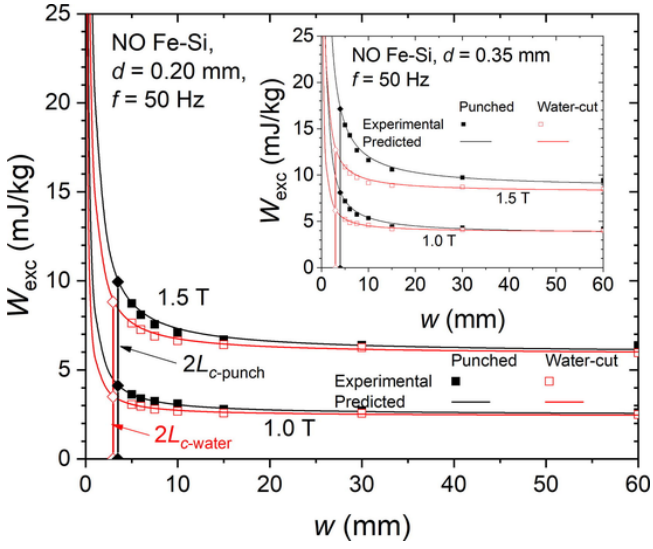

Fig. 6. Excess loss W_{exc} versus strip width w in 0.20 mm and 0.35 mm (inset) thick NO Fe-Si alloy (f = 50 Hz, J_p = 1.0 T and 1.5 T). The experimental W_{exc} values (symbols) are fitted by Eq. (6) (solid lines). Diamond symbols indicate the $2L_c$ limit.

ent degree of damage with respect to mechanical cutting.

Declaration of Competing Interest

The authors declare that they have no known competing financial interests or personal relationships that could have appeared to influence the work reported in this paper.

References

[1] International Energy Agency statistics, http://www.iea.org/stats, 2006.
[2] C.M. Gheorghe, S. Piperca, The induction machine in Eastern Europe: A research agenda, Rev. Roum. Sci. Techn. – Électrotechn. et Énerg. 63 (2018) 371–378.
[3] Y. Kurosaki, H. Mogi, H. Fujii, T. Kubota, M. Shiozaki, Importance of punching and workability in non-oriented electrical steel sheets, J. Magn. Magn. Mater. 320 (2008) 2474–2480, doi:10.1016/j.jmmm.2008.04.073.
[4] A. Kedous-Lebouc, O. Messal, A. Youmssi, Joint punching and frequency effects on practical magnetic characteristics of electrical steels for high-speed machines, J. Magn. Magn. Mater. 426 (2017) 658–665, doi:10.1016/j.jmmm.2016.10.150.
[5] Y. Zhang, Y. Xu, H. Liu, C. Li, G. Cao, Z. Liu, G. Wang, Microstructure, texture and magnetic properties of strip-cast 1.3% Si non-oriented electrical steel, J. Magn. Magn. Mater. 324 (2012) 3328–3333, doi:10.1016/j.jmmm.2012.05.046.
[6] P. Ghosh, R.R. Chromik, A.M. Knight, S.G. Wakade, Effect of metallurgical factors on the bulk magnetic properties of non-oriented electrical steels, J. Magn. Magn. Mater. 324 (2014) 42–51, doi:10.1016/j.jmmm.2013.12.052.
[7] K.M. Lee, M.Y. Huh, H.J. Lee, J.T. Park, J.S. Kim, E.J. Shin, O. Engler, Effect of hot band grain size on development of textures and magnetic properties in 2.0% Si non-oriented electrical steel sheet, J. Magn. Magn. Mater. 396 (2015) 53–64, doi:10.1016/j.jmmm.2015.08.010.
[8] Y. He, E.J. Hilinski, Texture and magnetic properties of non-oriented electrical steels processed by an unconventional cold rolling scheme, J. Magn. Magn. Mater. 405 (2016) 337–352, doi:10.1016/j.jmmm.2015.12.057.
[9] R. Ramadan, S.A. Ibrahim, M. Farag, A.A. Elzatahry, M.H. Es-Saheb, Processing optimization and characterization of magnetic non-oriented electrical silicon steel, Int. J. Electrochem. Sci. 7 (2012) 3242–3251.
[10] F.J.G. Landgraf, J.C. Teixeira, M. Emura, M.F. de Campos, C.S. Muranaka, Separating components of the hysteresis loss of non-oriented electrical steels, Mater. Sci. Forum 302–303 (1999) 440–445.
[11] F. Bohn, A. Gundel, F.J.G. Landgraf, A.M. Severino, R.L. Sommer, Magnetostriction in non-oriented electrical steels, Physica B 384 (2006) 294–296, doi:10.1016/j.physb.2006.06.014.
[12] X. Xiong, S. Hu, K. Hu, S. Zeng, Texture and magnetic property evolution of non-oriented Fe-Si steel due to mechanical cutting, J. Magn. Magn. Mater. 401 (2016) 982–990, doi:10.1016/j.jmmm.2015.10.023.
[13] N. Leuning, S. Elfgen, B. Groschup, G. Bavendiek, S. Steentjes, K. Hameyer, Advanced soft- and hard-magnetic material models for the numerical simulation of electrical machines, IEEE Trans. Magn. 54 (2018) 8107008, doi:10.1109/TMAG.2018.2865096.
[14] H.A. Weiss, N. Leuning, S. Steentjes, K. Hameyer, T. Andorfer, S. Jenner, W. Volk, Influence of shear cutting parameters on the electromagnetic properties of non-oriented electrical steel sheets, J. Magn. Magn. Mater. 421 (2017) 250–259, doi:10.1016/j.jmmm.2016.08.002.
[15] H. Cao, L. Hao, J. Yi, X. Zhang, Z. Luo, S. Chen, R. Li, The influence of punching process on residual stress and magnetic domain structure of non-oriented silicon steel, J. Magn. Magn. Mater. 406 (2016) 42–47, doi:10.1016/j.jmmm.2015.12.098.
[16] W. Wu, H. Cao, H. Ou, Z. Chen, X. Zhang, Z. Luo, S. Chen, R. Li, Effects of punching process on crystal orientations, magnetic and mechanical properties in non-oriented silicon steel, J. Magn. Magn. Mater. 444 (2017) 211–217, doi:10.1016/j.jmmm.2017.07.003.
[17] G. Paltanea, V. Manescu-Paltanea, H. Gavrila, A. Nicolaide, B. Dumitrescu, Comparison between magnetic industrial frequency properties of non-oriented FeSi alloys, cut by mechanical and water jet technologies, Rev. Roum. Sci. Techn. – Série Électrotechnique et Énergétique 61 (2016) 26–31.
[18] M. Bali, H. De Gersem, A. Muetze, Determination of original nondegraded and fully degraded magnetic characteristics of material subjected to laser cutting, IEEE Trans. Ind. Appl. 53 (2017) 4242–4251, doi:10.1109/TIA.2017.2696479.
[19] M. Petrun, S. Steentjes, K. Hameyer, D. Dolinar, Modeling the influence of varying magnetic properties in soft magnetic materials on the hysteresis shape using the flux tube approach, J. Appl. Phys. 117 (2015) 17A708, doi:10.1063/1.4906956.
[20] R. Siebert, J. Schneider, E. Beyer, Laser cutting and mechanical cutting of electrical steels and its effect on the magnetic properties, IEEE Trans. Magn. 50 (2014) 2001904, doi:10.1109/TMAG.2013.2285256.
[21] H.A. Weiss, S. Steentjes, P. Tröber, N. Leuning, T. Neuwirth, M. Schulz, K. Hameyer, R. Golle, W. Volk, Neutron grating interferometry investigation of punching-related local magnetic property deteriorations in electrical steels, J. Magn. Magn. Mater. 474 (2019) 643–653, doi:10.1016/j.jmmm.2015.12.057.
[22] V. Manescu-Paltanea, G. Paltanea, I.V. Nemoianu, Degradation of static and dynamic magnetic properties of non-oriented steel sheets by cutting, IEEE Trans. Magn. 54 (2018) 2001705, doi:10.1109/TMAG.2018.2834375.
[23] H. Zhao, E. Ferrara, V. Manescu (Paltanea), G. Paltanea, H. Gavrila, F. Fiorillo, Effect of punching and water-jet cutting methods on magnetization curve and energy losses of non-oriented magnetic steel sheets, Int. J. Appl. Electrom. 55 (2017) 69–76, doi:10.3233/JAE-172259.
[24] F. Fiorillo, Measurement and Characterization of Magnetic Materials, Elsevier Academic Press, 2004.
[25] G. Bertotti, Hysteresis in Magnetism, Elsevier Academic Press, 1998.
[26] C. Ragusa, H. Zhao, C. Appino, M. Khan, O. de la Barriere, F. Fiorillo, Loss decomposition in non-oriented steel sheets: the role of the classical losses, IEEE Magn. Lett. 7 (2016) 5106105, doi:10.1109/LMAG.2016.2604204.
[27] E. Barbisio, F. Fiorillo, C. Ragusa, Predicting loss in magnetic steels under arbitrary induction waveform and with minor hysteresis loops, IEEE Trans. Magn. 40 (2004) 1810–1819, doi:10.1109/TMAG.2004.830510.
[28] G. Bertotti, Physical interpretation of eddy current losses in ferromagnetic materials. II. Analysis of experimental results, J. Appl. Phys. 57 (1985) 2118–2126, doi:10.1063/1.334405.